Temperature dependence of the shifts and broadenings of the critical points in GaAs

Sudha Gopalan, P. Lautenschlager, and M. Cardona
Max-Planck-Institut für Feskörperforschung,
Heisenbergstrasse 1, D-7000 Stuttgart 80, Federal Republic of Germany
(Received 17 November 1986)

We present calculations of the shifts of the electronic states and their lifetime broadening with temperature in GaAs. The Debye-Waller and self-energy terms of the deformation-potential-type electron-phonon interaction are considered. The self-energy term is complex; its real part partly cancels the shifts caused by the Debye-Waller term and the imaginary part is responsible for the lifetime broadening. Results are obtained for the interband critical points E_0, E_0', E_1, and E_2 in GaAs. The shifts of these gaps, when corrected for the contribution of thermal expansion, show good agreement with ellipsometric data. The broadening of E_0' and E_2 gaps are underestimated when compared to the experimental results while the broadening of the E_1 gap is consistent with experiment.

I. INTRODUCTION

The various electronic states and interband critical points of semiconductors exhibit large shifts along with increasing lifetime broadening as the temperature is increased at constant pressure. These effects have been recently investigated in GaAs by studying the structures in the dielectric function obtained by ellipsometric techniques.[1] Several critical points labeled E_0, $E_0+\Delta_0$, E_0', E_1, $E_1+\Delta_1$, and E_2 were studied in great detail and their shifts and broadenings with temperature were analyzed with the empirical Varshni formula[2] or with an expression proportional to the Bose-Einstein occupation factor for the number of phonons, both containing several fitting parameters.

A microscopic analysis of these temperature-dependent shifts and broadenings rests on the renormalization of band energies by electron-phonon coupling.[3] A perturbative calculation[4] of the electron self-energy to second order in the atomic displacement **u** gives rise to two terms, the Debye-Waller[5] and the Fan or "self-energy"[6] terms whose Feynman diagrams are shown in Fig. 1. The Debye-Waller correction is an effect of the second-order electron-phonon interaction taken to first order in perturbation theory while the self-energy term is a first-order electron-phonon interaction taken to second order in perturbation theory. In addition, thermal expansion of the lattice, which causes changes in the electronic energies with volume, also contributes to the shifts of critical points. These terms have been calculated for various optical transitions in Si and Ge, and good agreement for both the shifts[7-9] and the broadenings[10] have been obtained with experimental results.

The microscopic treatment used with much success in group-IV semiconductors like Si and Ge is extended here to III-V semiconductors and results are computed for GaAs. Earlier calculations[11-13] of temperature shifts in GaAs completely ignored the Fan or "self-energy" term because it required tedious numerical computations. The earlier studies only took into account the softening of the pseudopotential form factors by the temperature-dependent Debye-Waller terms and the thermal expansion effects evaluated from the pressure dependence of the gaps. These results,[11] however, overestimate the shift of the E_0 gap in GaAs by about 60 meV when the temperature is raised from 0 to 300 K.[14] Further improvement in the pseudopotential parameters[13] did not significantly change this discrepancy. Very recently Kim *et al.*[15] included the self-energy term in addition to the terms described above and exactly eliminated the discrepancy of 60 meV at 300 K for the E_0 gap in GaAs. We present here calculations for the temperature shifts at various critical points and obtain good agreement with the experimental results.[1] We also compute the lifetime broadenings at all these points.

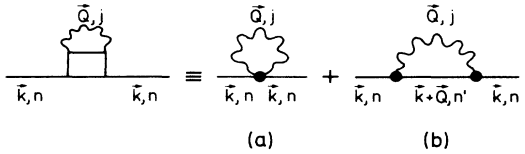

FIG. 1. Self-energy graphs which give the temperature renormalization of the band energies to second order in the atomic displacement; (a) represents the lowest-order Debye-Waller correction and (b) represents the Fan term.

II. THEORY

We follow the same treatment here as presented before for Si and Ge.[7-10] We repeat only the most important equations and point out those which are different. The renormalization of the unperturbed band energy $\varepsilon_{\mathbf{k}n}$ (of the state $|\mathbf{k}n\rangle$ with wave vector **k** and band index n) by the electron-phonon interaction (see Fig. 1) can be written as

$$E_{\mathbf{k}n}(T)=\varepsilon_{\mathbf{k}n}+\Delta_{\mathbf{k}n}^{\mathrm{DW}}+\Delta_{\mathbf{k}n}^{\mathrm{SE}}+i\Gamma_{\mathbf{k}n}\ , \tag{1}$$

where $\Delta_{\mathbf{k}n}^{\mathrm{DW}}$ is the shift of the band energy induced by the

Debye-Waller (DW) term. The complex self-energy (SE) term has a real part $\Delta_{\mathbf{k}n}^{\mathrm{SE}}$ which gives rise to an energy shift of the band states, and an imaginary part $\Gamma_{\mathbf{k}n}$, which causes a lifetime broadening of these states. We focus our attention here on the evaluation of all these terms for different states in GaAs.

All phonon modes $(\mathbf{Q},j)$ of energy $\omega_{\mathbf{Q}j}$ contribute to the energy shift and broadening:

$$\Delta E_{\mathbf{k}n}(T)=\sum_{\mathbf{Q},j}\frac{\partial E_{\mathbf{k}n}}{\partial n_{\mathbf{Q}j}}[n_{\mathbf{Q}j}(T)+\tfrac{1}{2}]\ , \tag{2}$$

where $n_{\mathbf{Q}j}$ is the Bose-Einstein occupation factor $(e^{\beta\omega_{\mathbf{Q}j}}-1)^{-1}$ with $\beta=1/k_BT$. The real part of the coefficient $\partial E_{\mathbf{k}n}/\partial n_{\mathbf{Q}j}$ contributing to the energy shift is the sum of the DW and SE parts, given by

$$\left[\frac{\partial E_{\mathbf{k}n}}{\partial n_{\mathbf{Q}j}}\right]_{\mathrm{SE}}=\frac{\hbar}{N}\sum_{\kappa,\kappa',n'}\frac{\left\langle \mathbf{k}n\left|\frac{\partial V}{\partial R_\alpha(\kappa)}\right|\mathbf{k}+\mathbf{Q}n'\right\rangle\left\langle \mathbf{k}+\mathbf{Q}n'\left|\frac{\partial V}{\partial R_\beta(\kappa')}\right|\mathbf{k}n\right\rangle}{\varepsilon_{\mathbf{k}n}-\varepsilon_{\mathbf{k}+\mathbf{Q}n'}}e^{-i\mathbf{Q}\cdot(\tau_\kappa-\tau_{\kappa'})}(M_\kappa M_{\kappa'}\omega_{\mathbf{Q}j}^2)^{-1/2}\epsilon_\alpha(-\mathbf{Q}j\kappa)\epsilon_\beta(\mathbf{Q}j\kappa')\ , \tag{3}$$

$$\left[\frac{\partial E_{\mathbf{k}n}}{\partial n_{\mathbf{Q}j}}\right]_{\mathrm{DW}}=-\frac{\hbar}{2N}\sum_{\kappa,\kappa',n'}\frac{\left\langle \mathbf{k}n\left|\frac{\partial V}{\partial R_\alpha(\kappa)}\right|\mathbf{k}n'\right\rangle\left\langle \mathbf{k}n'\left|\frac{\partial V}{\partial R_\beta(\kappa')}\right|\mathbf{k}n\right\rangle}{\varepsilon_{\mathbf{k}n}-\varepsilon_{\mathbf{k}n'}}$$
$$\times[(M_\kappa\omega_{\mathbf{Q}j})^{-1}\epsilon_\alpha(-\mathbf{Q}j\kappa)\epsilon_\beta(\mathbf{Q}j\kappa)+(M_{\kappa'}\omega_{\mathbf{Q}j})^{-1}\epsilon_\alpha(-\mathbf{Q}j\kappa')\epsilon_\beta(\mathbf{Q}j\kappa')]\ , \tag{4}$$

where M_κ is the mass of the atom κ located in the unit cell at position τ_κ, N is the number of unit cells in the crystal. $\partial V/\partial R_\alpha(\kappa)$ is the derivative of the atomic potential of the κth atomic species with respect to position R_α, the subscripts α and β denote Cartesian components which are summed when repeated, and $\epsilon(\mathbf{Q}j\kappa)$ is the polarization vector for the phonons $\mathbf{Q}j$ of the atom κ. The imaginary part of the coefficient $(\partial E_{\mathbf{k}n}/\partial n_{\mathbf{Q}j})$ in Eq. (2), which contributes to the broadening of the states, is given by

$$\frac{\partial\Gamma_{\mathbf{k}n}}{\partial n_{\mathbf{Q}j}}=\frac{\pi\hbar}{N}\sum_{\kappa,\kappa',n'}\left\langle \mathbf{k}n\left|\frac{\partial V}{\partial R_\alpha(\kappa)}\right|\mathbf{k}+\mathbf{Q}n'\right\rangle\left\langle \mathbf{k}+\mathbf{Q}n'\left|\frac{\partial V}{\partial R_\beta(\kappa')}\right|kn\right\rangle$$
$$\times e^{-i\mathbf{Q}\cdot(\tau_\kappa-\tau_{\kappa'})}(M_\kappa M_{\kappa'}\omega_{\mathbf{Q}j}^2)^{-1/2}\epsilon_\alpha(-\mathbf{Q}j\kappa)\epsilon_\beta(\mathbf{Q}j\kappa')\delta(\varepsilon_{\mathbf{k}n}-\varepsilon_{\mathbf{k}+\mathbf{Q}n'})\ . \tag{5}$$

In order to obtain the electronic states we use the local empirical pseudopotential method. The electronic states are then eigenvectors of the secular equations

$$\sum_{\mathbf{G}'}\left[\left[\frac{\hbar^2}{2m}(\mathbf{k}+\mathbf{G})^2-\varepsilon_{\mathbf{k}n}\right]\delta_{\mathbf{G}\mathbf{G}'}+\sum_\kappa V_\kappa(\mathbf{G}-\mathbf{G}')S_\kappa(\mathbf{G}-\mathbf{G}')\right]C_{\mathbf{k}n}(\mathbf{G}')=0\ , \tag{6a}$$

$$\Psi_{\mathbf{k}n}=\frac{1}{\Omega_c^{1/2}}\sum_{\mathbf{G}}C_{\mathbf{k}n}(\mathbf{G})e^{i(\mathbf{k}+\mathbf{G})\cdot\mathbf{r}}\ , \tag{6b}$$

$$\sum_{\mathbf{G}}|C_{\mathbf{k}n}(\mathbf{G})|^2=1\ , \tag{6c}$$

where Ω_c is the volume of the unit cell and $V_\kappa(\mathbf{G})$ and $S_\kappa(\mathbf{G})$ are, respectively, the local pseudopotential form factor and the structure factor of the atom κ in the unit cell. Because the masses of the two atoms in the unit cell are not the same, Eqs. (3)—(5) could not be reduced to the simplified forms for Si and Ge. Using Eq. (6) and the rigid-ion model we finally obtain the following contributions for the shifts:

$$\left[\frac{\partial E_{\kappa n}}{\partial n_{\mathbf{Q}j}}\right]_{\mathrm{SE}}=\sum_{n',\kappa}\frac{\left|\mathbf{A}(\mathbf{k},n,n',\mathbf{Q},\kappa)\cdot\frac{\epsilon(-\mathbf{Q}j\kappa)}{(M_\kappa)^{1/2}}\right|^2}{\varepsilon_{\mathbf{k}n}-\varepsilon_{\mathbf{k}+\mathbf{Q}n'}}\ , \tag{7}$$

$$\left[\frac{\partial E_{\mathbf{k}n}}{\partial n_{\mathbf{Q}j}}\right]_{\mathrm{DW}}=-\tfrac{1}{2}\sum_{n',\kappa,\kappa'}\frac{A_\alpha^*(\mathbf{k},n,n',0,\kappa)A_\beta(\mathbf{k},n,n',0,\kappa')}{\varepsilon_{\mathbf{k}n}-\varepsilon_{\mathbf{k}n'}}\left[\frac{1}{M_\kappa}\epsilon_\alpha(-\mathbf{Q}j\kappa)\epsilon_\beta(\mathbf{Q}j\kappa)+\frac{1}{M_{\kappa'}}\epsilon_\alpha(-\mathbf{Q}j\kappa')\epsilon_\beta(\mathbf{Q}j\kappa')\right]\ , \tag{8}$$

while the broadening term gives

$$\frac{\partial\Gamma_{\mathbf{k}n}}{\partial n_{\mathbf{Q}j}}=\pi\sum_{n',\kappa}\left|\mathbf{A}(\mathbf{k},n,n',\mathbf{Q},\kappa)\cdot\frac{\boldsymbol{\epsilon}(-\mathbf{Q}j\kappa)}{(M_\kappa)^{1/2}}\right|^2 \times\delta(\varepsilon_{\mathbf{k}n}-\varepsilon_{\mathbf{k}+\mathbf{Q}n'}) , \tag{9}$$

where

$$A_\alpha(\mathbf{k},n,n',\mathbf{Q},\kappa)=\sum_{\mathbf{G},\mathbf{G}'}\left[\frac{\hbar}{\omega_{\mathbf{Q}j}}\right]^{1/2}C^*_{\mathbf{k}+\mathbf{Q}n'}(\mathbf{G}')C_{\mathbf{k}n}(\mathbf{G}) \times(\mathbf{G}'-\mathbf{G}+\mathbf{Q})_\alpha V_\kappa(\mathbf{G}'-\mathbf{G}+\mathbf{Q})e^{-i(\mathbf{G}'-\mathbf{G})\cdot\tau_\kappa} . \tag{10}$$

It has been verified that all these equations reduce to those for Si and Ge when the masses of the two atoms in the unit cell are identical.

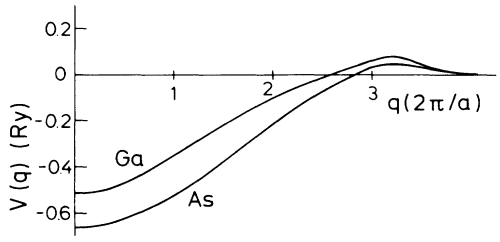

FIG. 2. Local pseudopotential form factors $V(q)$ for Ga and As used in the band-structure calculation, which were interpolated using the values of Ref. 18.

III. NUMERICAL PROCEDURE

In order to obtain numerical estimates of the temperature dependence of the electronic states and their broadening we rewrite Eq. (2) as

$$\Delta E_{\mathbf{k}n}(T)=\int_0^\infty d\Omega\, g^2F(k,n,\Omega)[n_{\mathbf{Q}j}(T)+\tfrac{1}{2}] , \tag{11}$$

TABLE I. Electron-phonon coupling coefficients as defined by Eqs. (7) and (8) for states at $\mathbf{k}=\mathbf{0}$ and phonons at points X and L. In addition to the total sum over all intermediate states, the Debye-Waller and the self-energy contributions from the lowest eight intermediate states are listed separately. The figures in the parentheses are the corresponding values for Ge.

Initial state	Intermediate state	Coefficients $\partial E_{\mathbf{k}n}/\partial n_{\mathbf{Q}j}$ (meV) for X-point phonons X_5(TA)	X_1(LA)	X_3(LO)	X_5(TO)
$\Gamma_{15}(v)$	$X_1(v)$	2.0(0)	1.0(0.9)	4.2(0.9)	4.7(3.6)
	$X_3(v)$	0.4(0)	0.4(0.9)	0(0.9)	2.5(3.6)
	$X_5(v)$	0(0)	6.0(5.3)	3.4(5.3)	2.5(3.0)
	$X_1(c)$	−9.3(−9.5)	0(−2.5)	−11.7(−2.5)	−0.7(0)
	$X_3(c)$	−16.6(−9.5)	−0.7(−2.5)	0(−2.5)	−1.8(0)
	$X_5(c)$	−0.2(0)	0(−0.7)	−1.4(−0.7)	−1.0(−1.3)
	DW	20.6(18.8)	2.6(6.7)	10.8(6.7)	5.7(5.8)
	Total	−7.6(−2.1)	12.9(10.4)	3.7(10.4)	9.2(12.7)
$\Gamma_1(c)$	$X_1(v)$	0(0)	0(0)	0(0)	0(0)
	$X_3(v)$	0(0)	0(0)	0(0)	0(0)
	$X_5(v)$	0.2(0)	0(0)	0(0)	0(0)
	$X_1(c)$	0(0)	−29.7(9.2)	0(9.2)	0(0)
	$X_3(c)$	0(0)	0(9.2)	−3.9(9.2)	0(0)
	$X_5(c)$	−0.7(1.4)	0(0)	0(0)	−0.2(0)
	DW	−1.0(−2.0)	−0.7(−0.7)	0(−0.7)	−0.3(−0.6)
	Total	−4.5(−5.8)	−30.8(17.1)	−6.7(17.1)	−3.8(−2.7)
$\Gamma_{15}(v)$	$L_1(v)$	3.6(0)	0.5(0.6)	3.3(0)	4.1(4.0)
	$L_1(v)$	0(0)	0.2(0)	4.5(7.2)	0.2(0)
	$L_3(v)$	0.3(0)	9.7(9.1)	0(0)	19.3(21.2)
	$L_1(c)$	−8.9(−8.6)	−1.1(0)	−6.7(−5.8)	−0.4(0)
	$L_3(c)$	−8.3(−8.3)	0(0)	−0.5(−0.5)	−1.1(0)
	$L_1(c)$	0(0)	0(0)	0(0)	0(0)
	DW	27.2(25.9)	5.3(7.5)	8.7(6.6)	5.2(5.4)
	Total	0.1(−4.0)	23.4(24.8)	0.5(0.2)	41.9(48.5)
$\Gamma_1(c)$	$L_1(v)$	0(0)	0(0)	0(0)	0(0)
	$L_1(v)$	0(0)	0.1(0.1)	0(0)	0(0)
	$L_3(v)$	0.8(0.7)	0(0)	0(0)	0(0)
	$L_1(c)$	0(0)	−23.5(26.1)	0(0)	0(0)
	$L_3(c)$	0(0)	0(0)	0(0)	−0.5(−0.6)
	$L_1(c)$	0(0)	0(0)	−0.4(−0.2)	0(0)
	DW	−1.0(−2.8)	−0.6(−0.8)	−0.2(−0.7)	−0.4(−0.6)
	Total	−5.2(−6.7)	−24.5(25.0)	−4.5(−2.3)	−3.5(−3.0)

where

$$g^2F(\mathbf{k},n,\Omega)=\sum_{Q,j}\frac{\partial E_{kn}}{\partial n_{Qj}}\delta(\Omega-\omega_{Qj})\ . \tag{12}$$

Here $g^2F(\mathbf{k},n,\Omega)$ is a temperature-independent electron-phonon spectral function. It corresponds to the density of phonon states weighted by appropriate electron-phonon matrix elements.

We first compute $g^2F(\mathbf{k},n,\Omega)$ for the DW and SE contributions, and the broadening for various valence- and conduction-band states using the tetrahedron method.[16,17] The irreducible $\frac{1}{48}$ wedge of the Brillouin zone is divided into 228 small tetrahedra which corresponds to a discrete mesh of 89 **k** points.[8–10] The band structure was obtained from Eq. (6) with a basis of 59 plane waves and using smoothly varying pseudopotential curves for Ga and As as shown in Fig. 2. These curves were obtained by interpolating Cohen-Bergstresser's[18] form factors and extrapolating to $V(0)=-\frac{2}{3}\varepsilon_F$, with ε_F equal to the free-electron Fermi energy of the valence electrons. We have disregarded here the spin-orbit interaction. The phonon frequencies and eigenvectors were calculated using the shell-model program of Kunc and Nielson.[19,20] The remaining details are the same as described in Refs. 8–10.

In order to facilitate comparison with the experimental data, the calculations were done for the following optical transitions in GaAs: the direct gap E_0 ($\Gamma_{15}-\Gamma_1$), the second direct gap E_0', both transitions occurring at the Γ point of the Brillouin zone, the E_1 gap, which corresponds to transitions between $(2\pi/a)(\frac{1}{4},\frac{1}{4},\frac{1}{4})$ and $(2\pi/a)(\frac{1}{2},\frac{1}{2},\frac{1}{2})$, and the E_2 gap. The region where the E_2 transition takes place is not very well defined; we use the point $(2\pi/a)(\frac{3}{4},\frac{1}{4},\frac{1}{4})$ as the representative point.[21]

One important check of the numerical procedure is the direct calculation of the Debye-Waller contribution. This is very easily done by replacing the zero-temperature structure factor $S(G)$ in the secular Eq. (6) by

$$S(\mathbf{G})\exp(-|G|^2\langle u^2\rangle/6)\ , \tag{13}$$

where $\langle u^2\rangle$ is the mean-square thermal amplitude. The recent calculation of Kim *et al.*[15] took the values of $\langle u^2\rangle_{As}$ and $\langle u^2\rangle_{Ga}$ to be the same. This was so assumed

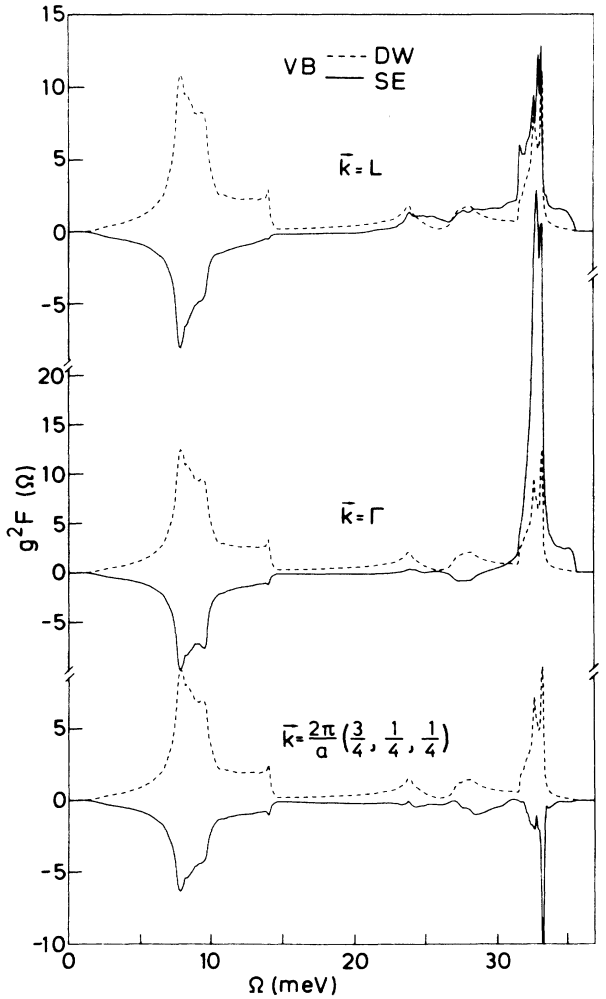

FIG. 3. Dimensionless spectral functions $g^2F(\Omega)$ which give rise to the temperature shifts of the highest valence-band states (VB). Both the DW (dashed line) and SE (solid line) contributions at several **k** points are shown.

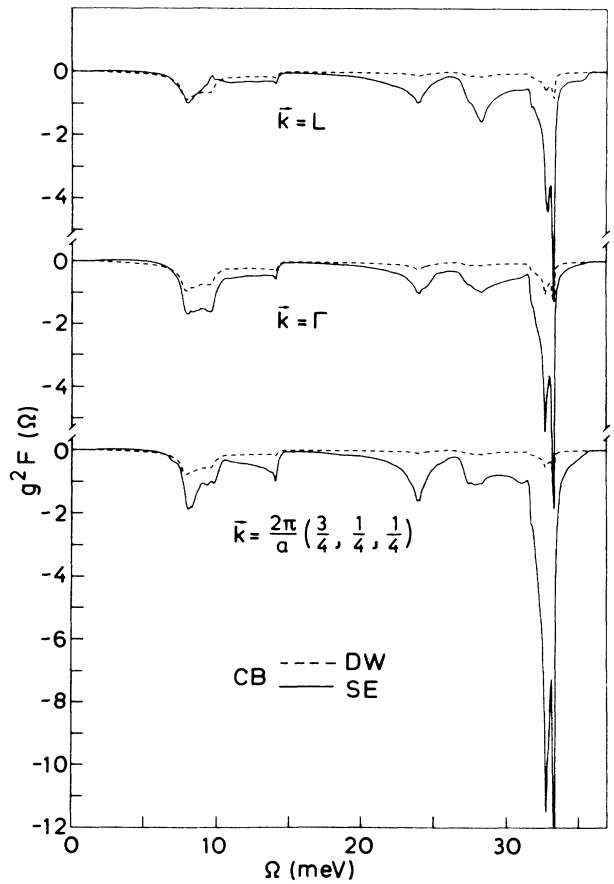

FIG. 4. DW (dashed line) and SE (solid line) parts of the spectral functions $g^2F(\Omega)$ which give rise to temperature shifts of the lowest conduction-band states (CB) shown for several **k** points.

TABLE II. Data used for the calculation of the thermal shift of band gaps with Eq. (14).

Parameter		Values	Refs.
B (GPa)		76	21
$\left[\frac{\partial E_g}{\partial p}\right]_T$ (meV/GPa)	E_0'	9.9	23
	E_1	76	21
	E_2	57	21

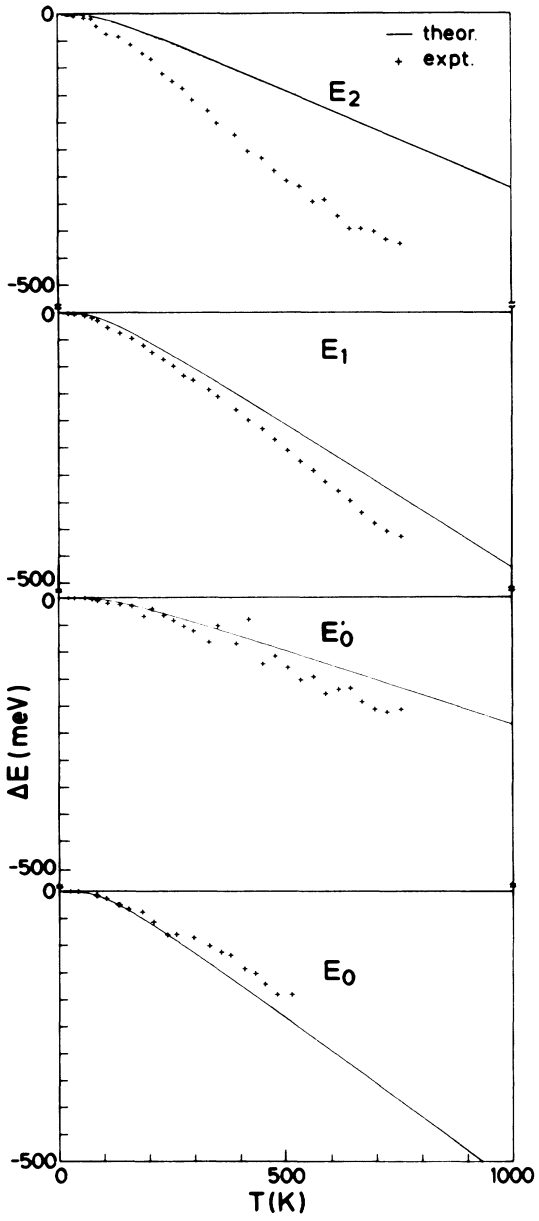

FIG. 5. Temperature dependence of the interband critical points E_0, E_0', E_1, and E_2 of GaAs. Solid lines give the total calculated shifts due to electron-phonon interaction plus thermal expansion, the experimental points (+) were obtained by ellipsometry measurements (Ref. 1).

because the 14-parameter shell model of Dolling and Waugh,[20] which we have also used here, gives $\langle u^2\rangle_{Ga} < \langle u^2\rangle_{As}$, in disagreement with experiments.[22] By doing band-structure calculations with this temperature-dependent structure factor [Eq. (6)] and using the experimental values of $\langle u^2\rangle_{Ga}$ obtained from Ref. 22, the shifts of the gaps agreed with the results obtained by perturbation theory only to within about 10%. This difference may be due to the non-self-consistent choice in the value of $\langle u^2\rangle_{As}$ used by Kim *et al.* Hence in all our present calculations we use the perturbative method [Eq. (8)] to calculate the Debye-Waller term.

IV. RESULTS

We first present the electron-phonon spectral functions $g^2F(\Omega)$ responsible for the temperature shifts of various electronic states $|\mathbf{k}n\rangle$. As mentioned before, these functions consist of DW and SE contributions, which are plotted in Figs. 3 and 4 for the valence and conduction bands,

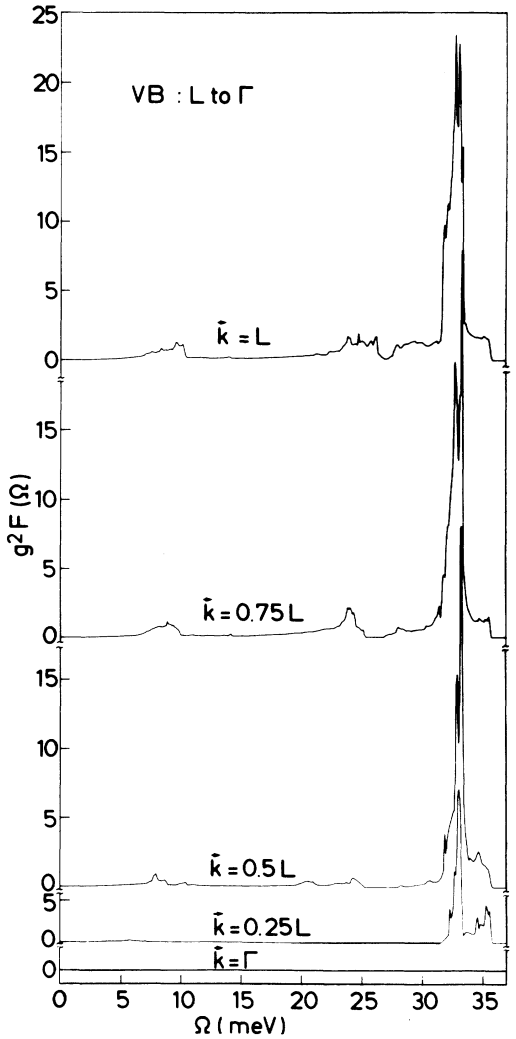

FIG. 6. Dimensionless spectral functions $g^2F(\Omega)$ responsible for the broadening of the highest valence-band states. A sequence of points from L to Γ is shown.

respectively, at various points in the Brillouin zone. All curves have two sharp peaks associated with the TA (centered at 8 meV) and the TO (centered at 33 meV). It is of interest to note that the general shape of the DW term at different k points remains the same for both the conduction and the valence bands. In the valence-band states the self-energy terms strongly suppress the acoustic phonon and enhance the optical phonon contributions from the Debye-Waller term, except at $\mathbf{k}=(2\pi/a)(\frac{3}{4},\frac{1}{4},\frac{1}{4})$, which corresponds to the E_2 structure. At this point, both the acoustic and the optical phonons are suppressed. For the conduction-band states, however, all the phonon contributions are enhanced by the self-energy term. Further insight into the behavior of these spectral functions can be obtained by examining contribution of individual phonons to intermediate electronic state. Table I gives such an analysis for X- and L-point phonons. The results are expressed in terms of the coupling coefficients $\partial E_{\mathbf{k}n}/\partial n_{Qj}$ as defined by Eqs. (7) and (8). When the phonon is doubly degenerate, the contribution shown is one-half that of the pair. Similarly, when the intermediate state is doubly degenerate, the contribution shown is half the total contribution of the doublet.

In order to obtain the temperature shift of band gaps the contributions from the Debye-Waller and the self-energy terms are added and the integration over all phonon energies, as shown in Eq. (11), is performed. In addition, the energy shift due to thermal expansion (TE) is calculated using[9]

$$\left[\frac{\partial E_g}{\partial T}\right]_{\mathrm{TE}} = -3\alpha B\left[\frac{\partial E_g}{\partial p}\right]_T , \tag{14}$$

where α is the thermal expansion coefficient and B the bulk modulus. In Table II we present the values of these constants and $(\partial E_g/\partial p)_T$ for the different critical points. The thermal expansion effect on the E_0 gap is evaluated using the experimental variation of E_0 with lattice constant a_0 (Refs. 15 and 24) given by

$$E_0(a_0+\Delta a_0)-E_0(a_0) = -29.3\frac{\Delta a_0}{a_0}-57.5\left[\frac{\Delta a_0}{a_0}\right]^2 (\mathrm{eV}) . \tag{15}$$

The change in a_0 with T is calculated using the thermal expansion data of Ref. 21. The contributions of all these terms are included to obtain the temperature shifts of the E_0, E_0', E_1, and E_2 gaps and the results are shown in Fig. 5 along with the experimental results. The agreement between theory and experiment is very good in all transitions except for the E_2 gap. It is, however, not clear to what extent the $\mathbf{k}=(2\pi/a)(\frac{3}{4},\frac{1}{4},\frac{1}{4})$ point is representa-

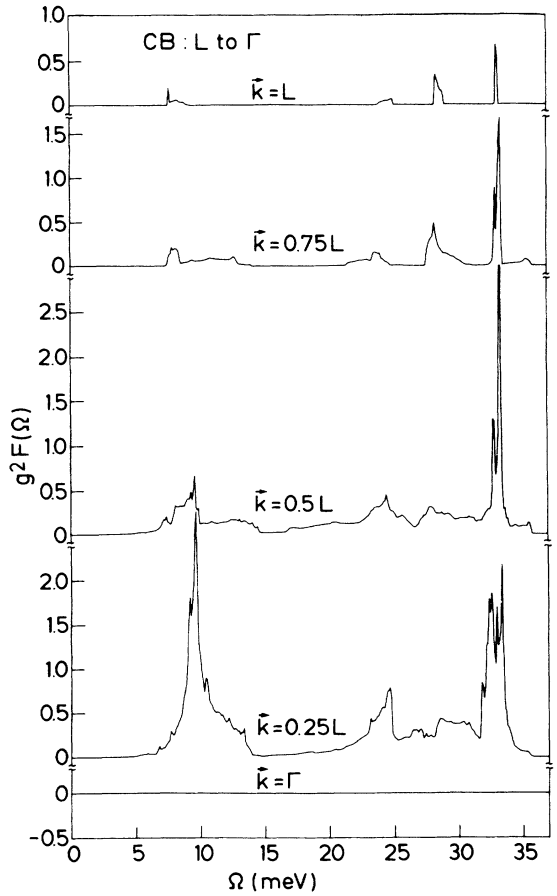

FIG. 7. Dimensionless spectral functions $g^2F(\Omega)$ responsible for the broadening of the lowest conduction-band states. A sequence of points from L to Γ is shown.

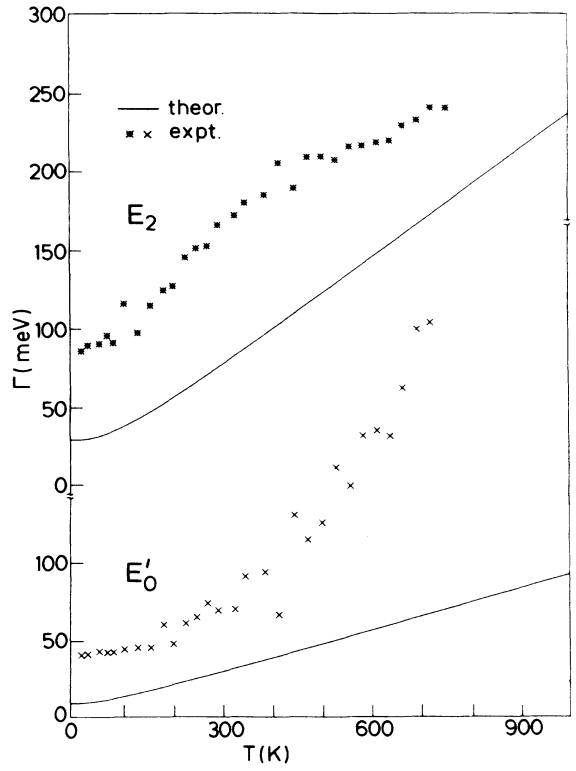

FIG. 8. Calculated temperature dependence of the broadenings of the E_0' and E_2 critical points of GaAs. The experimental points are from Ref. 1 obtained by a fit with a two-dimensional (2D) line shape.

tive of this gap.

We now discuss the broadenings of the various electronic states. We first present the calculated spectral function $g^2F(\Omega)$ using the coefficient $\partial\Gamma_{kn}/\partial n_{Qj}$ from Eq. (9). The results are shown in Figs. 6 and 7 for the valence and conduction bands for several **k** points going from Γ to L in the Brillouin zone. From Fig. 6 we note that the leading contribution to the valence-band states is from optical phonons. Small structure related to acoustic phonons is, however, also observed. For the conduction-band states in Fig. 7 we observe a marked contribution from acoustic phonons for $k=0.25L$. The zero-point broadening $\Gamma(0)$ is proportional to the area under $g^2F(\Omega)$. In the high-temperature limit there is a factor of $2k_BT/\hbar\Omega$ in the integrand that gives more weight to the low-frequency phonons. Hence a large contribution from acoustic phonons would produce a broadening that strongly increases with temperature.

In order to obtain the total broadening at the critical points, the broadening of the valence- and conduction-band states are added up. These results are shown in Figs. 8 and 9 for the gaps E_0', and E_2, and E_1, respectively. According to the present calculation the E_0 gap is not associated with any broadening. This is because the valence and conduction bands here are at the absolute maximum and minimum, respectively, and there are no other electronic states with the same energy. In our model we have neglected the phonon energies in the energy conservation, which appear in the δ function of Eq. (5). This implies that usually the electronic density of states does not vary much in less than 0.1 eV. If this assumption were lifted the band-edge states would broaden slightly through phonon absorption at $T\neq 0$, which indeed is observed experimentally.[1]

According to Fig. 8, the experimental broadening of the E_2 structure is larger than the calculated one by a nearly constant amount ($\sim$50 meV) at all temperatures: The temperature increase in Γ is well represented by the calculation. The additional increase may be due to the inadequate description of E_2 by a single critical point. Several critical points, separated by $\sim$50 meV, may result in the additional broadening when a fit to a single critical point is performed.

The broadening calculated for E_0' is also smaller than the measured one. The temperature increase is well represented by the calculations from 0 to 400 K but at higher temperatures an additional increase is found experimentally. This increase may be an artifact of the fit as the structure broadens and the signal-to-noise ratio decreases.

Figure 9 shows excellent agreement between calculations and the experimental data for fits with a two-dimensional critical point to the E_1 structure. The experimental results for a fit obtained with a Fano-type excitonic line are also shown.[1] The calculations represent well the change of Γ with temperature obtained from such a fit provided a constant broadening of 18 meV is added to the calculation.

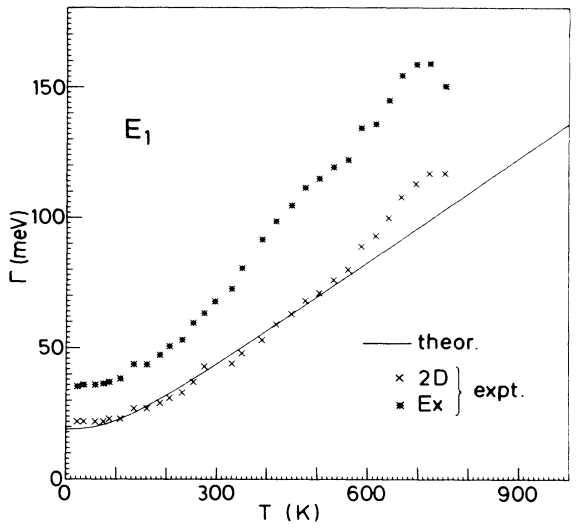

FIG. 9. Calculated temperature dependence of the broadenings of the E_1 gap of GaAs. The experimental points are from Ref. 1 obtained by a fit with an exitonic (*) and a 2D (×) line shape.

V. CONCLUSIONS

The rigid-ion pseudopotential model, used previously to obtain the self-energies of electronic states in Ge and Si has been generalized to GaAs, a polar material. Good agreement between the calculated real and imaginary parts of these self-energies with experimental data has been found. Since the calculations include only short-range (deformation-potential) electron-phonon interaction, we conclude that the long-range Fröhlich interaction is not important for the phenomenon treated here.

It would be of interest to use the calculated electron-phonon coupling constants to predict the strength of indirect optical interband transitions. These transitions should become observable upon application of high pressures such as those obtained in a diamond anvil cell. Also, the method could be used to calculate the strength of resonant Raman scattering by two phonons.[25]

ACKNOWLEDGMENT

We would like to thank P. B. Allen and C. K. Kim for a number of useful discussions.

[1]P. Lautenschlager, M. Garriga, S. Logothetidis, and M. Cardona (unpublished).
[2]Y. P. Varshni, Physica (Utrecht) **34**, 149 (1967).
[3]M. L. Cohen and D. J. Chadi, in *Semiconductor Handbook*, edited by M. Balkanski (North-Holland, Amsterdam, 1980), Vol. 2, Chap. 4b.
[4]P. B. Allen and V. Heine, J. Phys. C **9**, 2305 (1976).
[5]E. Antončik, Czech, J. Phys. **5**, 449 (1955).
[6]H. Y. Fan, Phys. Rev. **82**, 900 (1951).
[7]P. B. Allen and M. Cardona, Phys. Rev. B **23**, 1495 (1981).

[8]P. B. Allen and M. Cardona, Phys. Rev. B **27**, 4760 (1983).
[9]P. Lautenschlager, P. B. Allen, and M. Cardona, Phys. Rev. B **31**, 2163 (1985).
[10]P. Lautenschlager, P. B. Allen, and M. Cardona, Phys. Rev. B **33**, 5501 (1986).
[11]J. P. Walter, R. R. L. Zucca, M. L. Cohen, and Y. R. Shen, Phys. Rev. Lett. **24**, 102 (1970).
[12]Y. F. Tsay, B. Gong, S. S. Mitra, and J. F. Vetelino, Phys. Rev. B **6**, 2330 (1972).
[13]J. Camassel and D. Auvergne, Phys. Rev. B **12**, 3258 (1975).
[14]J. L. Shay, Phys. Rev. B **4**, 1385 (1971).
[15]C. K. Kim, P. Lautenschlager, and M. Cardona, Solid State Commun. **59**, 797 (1986).
[16]G. Lehmann and M. Taut, Phys. Status Solidi B **54**, 469 (1973).
[17]P. B. Allen, Phys. Status Solidi B **120**, 529 (1983).
[18]M. L. Cohen and T. K. Bergstresser, Phys. Rev. **141**, 789 (1966).
[19]K. Kunc and O. H. Nielsen, Comput. Phys. Commun. **16**, 181 (1979); **17**, 413 (1979).
[20]G. Dolling and J. L. T. Waugh, in *Lattice Dynamics,* edited by R. F. Wallis (Pergamon, Oxford, 1965), pp. 19—32.
[21]*Physics of Group IV Elements and III-V Compounds,* Group III, Vol. 17a of *Landolt-Börnstein Tables,* edited by O. Madelung (Springer, Berlin, 1982).
[22]J. S. Reid, Acta Crystallogr. A **39**, 1 (1983).
[23]N. E. Christensen, Phys. Rev. B **30**, 5753 (1984).
[24]B. Welber, M. Cardona, C. K. Kim, and S. Rodriguez, Phys. Rev. B **12**, 5729 (1975).
[25]M. Cardona and P. B. Allen, Helv. Phys. Acta **58**, 307 (1985).